ACS APPLIED MATERIALS & INTERFACES

Research Article

www.acsami.org

A Cell-Surface-Anchored Ratiometric Fluorescent Probe for Extracellular pH Sensing

Guoliang Ke, Zhi Zhu,* Wei Wang, Yuan Zou, Zhichao Guan, Shasha Jia, Huimin Zhang, Xuemeng Wu, and Chaoyong James Yang*

State Key Laboratory of Physical Chemistry of Solid Surfaces, Collaborative Innovation Center of Chemistry for Energy Materials, the Key Laboratory for Chemical Biology of Fujian Province, The MOE Key Laboratory of Spectrochemical Analysis & Instrumentation, Department of Chemical Biology, College of Chemistry and Chemical Engineering, Xiamen University, Xiamen 361005, P. R. China

Supporting Information

ABSTRACT: Accurate sensing of the extracellular pH is a very important yet challenging task in biological and clinical applications. This paper describes the development of an amphiphilic lipid−DNA molecule as a simple yet useful cell-surface-anchored ratiometric fluorescent probe for extracellular pH sensing. The lipid−DNA probe, which consists of a hydrophobic diacyllipid tail and a hydrophilic DNA strand, is modified with two fluorescent dyes; one is pH-sensitive as pH indicator and the other is pH-insensitive as an internal reference. The lipid−DNA probe showed sensitive and reversible response to pH change in the range of 6.0−8.0, which is suitable for most extracellular studies. In addition, based on simple hydrophobic interactions with the cell membrane, the lipid−DNA probe can be easily anchored on the cell surface with negligible cytotoxicity, excellent stability, and unique ratiometric readout, thus ensuring its accurate sensing of extracellular pH. Finally, this lipid−DNA-based ratiometric pH indicator was successfully used for extracellular pH sensing of cells in 3D culture environment, demonstrating the potential applications of the sensor in biological and medical studies.

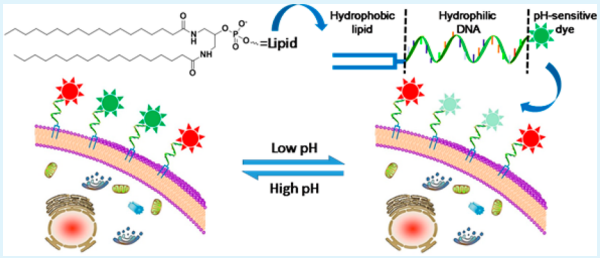

KEYWORDS: *extracellular pH sensing, lipid−DNA, ratiometric fluorescent probe, cell surface anchorage*

INTRODUCTION

The extracellular pH plays an important role in chemical reactions and biological processes.[1,2] For example, differing from the neutral extracellular pH of normal cells (7.2−7.4), the extracellular pH of tumor cells is reported to be acidic (6.2−6.9), which affects tumor properties, including adhesion, migration, and drug resistance. Therefore, it is of significance to develop techniques for accurate extracellular pH sensing.[3,4]

Compared to present measurement methods, including microelectrode, nuclear magnetic resonance, and absorption spectroscopy,[5,6] fluorescence-based techniques such as fluorescence microscopy have the advantages of high sensitivity, excellent spatiotemporal resolution, and high throughput, as well as wide applications in 3D and even in vivo biosensing.[7,8] The development of pH-sensitive fluorescent indicators is thus the primary task for fluorescence-based extracellular pH sensing. At present, although several new probes such as organic dyes,[8−10] nanoparticles,[7,11−16] and fluorescent proteins[17,18] have been developed, they act as intracellular rather than extracellular pH indicators due to their easy entry into cells.

Recently, a genetically encoded ratiometric sensor was developed for extracellular pH measurement. Via the translation of an exogenously introduced DNA sequence, a chimeric membrane protein consisting of a pH-sensitive yellow fluorescent protein and a pH-insensitive cyan fluorescent protein was expressed at the external aspect of the cell surface to detect the extracellular pH change.[19] This type of genetically encoded sensor provides the advantages of ratiometric measurement and cell-surface anchorage, but it suffers from the drawbacks of complex manipulation and large size. Thus, a cell-anchored ratiometric fluorescent sensor with small size, high sensitivity, reversible response, and excellent stability is desirable for extracellular pH measurement.

Herein, we report a novel lipid−DNA-based cell-surface-anchored ratiometric fluorescent probe for extracellular pH sensing. On the basis of hydrophobic interactions and the pH-sensitive dye, the probe can be easily anchored on cell surfaces with negligible cytotoxicity, excellent stability, and unique ratiometric readout, thus ensuring accurate sensing of extracellular pH. As a proof-of-concept, the new probe was successfully used for sensing of extracellular pH in 3D collagen gels, establishing it as a useful tool for extracellular pH sensing.

MATERIALS AND METHODS

DNA Synthesis. All oligonucleotides (Table 1) were synthesized on the basis of solid-phase phosphoramidite chemistry with DNA synthesis reagents (Glen Research) using a PolyGen DNA synthesizer

Received: June 16, 2014
Accepted: August 11, 2014
Published: August 11, 2014

Table 1. DNA Sequences Used in This Study

name	sequence
Lipid-T_{20}	5′-lipid-TTT TTT TTT TTT TTT TTT TT-3′
Lipid-T_{20}-FAM	5′-lipid-TTT TTT TTT TTT TTT TTT TT-FAM-3′
Lipid-T_{20}-TAMRA	5′-lipid-TTT TTT TTT TTT TTT TTT TT-TAMRA-3′
T_{20}	5′-TTT TTT TTT TTT TTT TTT TT-3′
A_{20}-FAM	5′-FAM-AAA AAA AAA AAA AAA AAA AA-3′
Ran-FAM	5′-FAM-AAG GAG CAG CGT GGA GGA TA-3′

Scheme 1. (A) Structure of the Lipid–DNA Probes and (B) Working Principle of Cell-Anchored Lipid–DNA Probes for Ratiometric Fluorescent Sensing of Extracellular pH

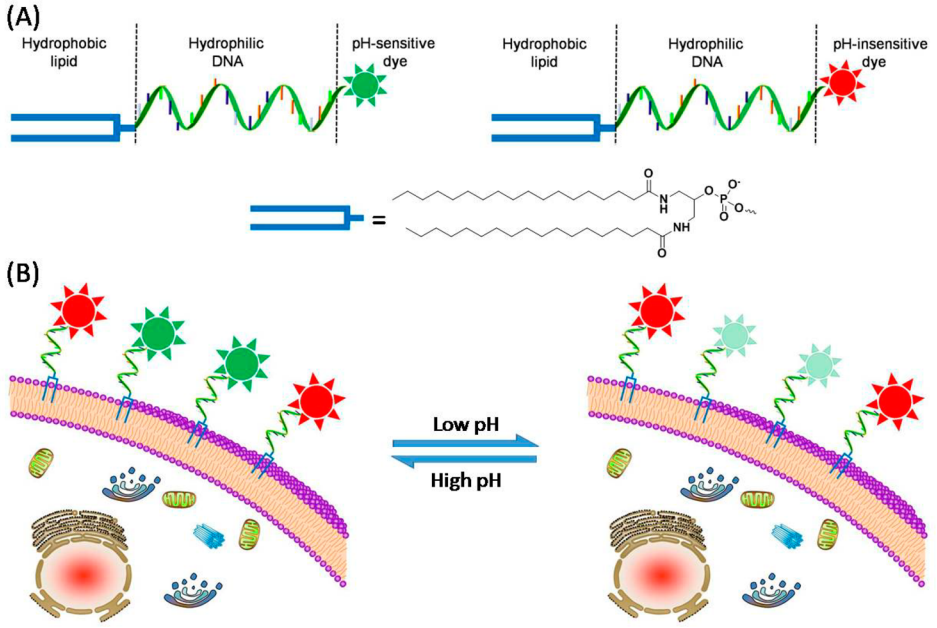

(PloyGen). Lipid phosphoramidite was synthesized according to previous reports,[20−22] and was directly coupled onto the sequences by the DNA synthesizer with an extended coupling time (900 s). The resulting lipid–DNA sequences were purified by reversed-phase HPLC using a C4 column (BioBasic-4, 200 mm × 4.6 mm, Thermo Scientific) with 100 mM triethylamine/acetic acid buffer (TEAA, pH 7.5) and acetonitrile (0–30 min, 10–100%) as the eluent.

Fluorescence Measurements in Buffer. Fluorescence measurements were carried out on a FluoroMax-4P fluorescence spectrophotometer (Horiba, Japan). Probes consisting of 100 nM Lipid-T_{20}-FAM and 100 nM Lipid-T_{20}-TAMRA were added to the extracellular environment monitoring phosphate buffers (10 mM phosphate, 140 mM NaCl, 5 mM KCl, 3 mM $MgCl_2$) containing 0.1 mg/mL 1,2-dioleoyl-*sn*-glycero-3-phosphocholine (DOPC)[8] with different pHs for a pH-sensitive fluorescent spectrum study. For each sample, the emission spectra of FAM and TAMRA were obtained by excitation at 488 nm (with emission wavelength from 500 to 545 nm) and 543 nm (with emission wavelength from 555 to 700 nm), respectively, with 3 nm bandwidth and 1 nm step length. The response curve of fluorescence ratio (F_{520nm}/F_{580nm}) and buffer pH was obtained through three independent experiments.

Cell Culture. Human cervical cancer cell line HeLa cells (American Type Culture Collection, ATCC), human liver cancer cells QGY-7703 (ATCC), human liver normal cells QSG-7701 (ATCC), and human acute T cell leukemia cells Jurkat (ATCC, an example of suspension cells) were grown in relevant medium (DMEM medium for HeLa and RPMI-1640 medium for others) containing 10% FBS (fetal bovine serum), penicillin (100 U/mL), and streptomycin (100 mg/mL) and cultured at 37 °C in 95% air/5% CO_2.

Confocal Fluorescence Microscopy Imaging. All cellular fluorescent images were collected with a TCS SP5 confocal laser-scanning microscope (Leica). FAM- or TAMRA-labeled probes were respectively excited at 488 nm (with emission wavelength from 500 to 540 nm) and 543 nm (with emission wavelength from 560 to 600 nm), while Hochest 33258 was excited at 405 nm (with emission wavelength from 460 to 500 nm). To study the location of lipid–DNA on the cell membrane, cells were incubated in serum-free medium containing 1 μM Lipid-T_{20}-FAM (or Lipid-T_{20}) for 2 h, followed by washing three times with PBS to remove unbound probes. For extracellular pH measurement, cells were incubated in serum-free medium containing 1 μM mixed lipid–DNA probes (Lipid-T_{20}-FAM:Lipid-T_{20}-TAMRA = 1:1) for 2 h, washed with PBS, and incubated in the extracellular environment to monitor phosphate buffers with different extracellular pH for confocal imaging. The imaging results were analyzed using ImageJ. Each point in the calibration curve was calculated by averaging the fluorescence ratio value of more than three cells.

Flow Cytometric Assay. To study the location of lipid–DNA on the cell membrane, HeLa cells were incubated with 1 μM unlabeled DNA probes (Lipid-T_{20} or T_{20}) for 2 h and washed with PBS buffer, followed by incubation with 2.5 μM FAM-labeled DNA probes (A_{20}-FAM or Ran-FAM) and washing to remove the unbound DNA probes. After treatment with trypsin, cells were suspended in PBS buffer for flow cytometric assay. For extracellular pH measurement, cells were incubated with 1 μM mixed lipid–DNA probes (Lipid-T_{20}-FAM:Lipid-T_{20}-TAMRA = 1:1) for 2 h, followed by washing three times with PBS to remove unbound probes. After treatment with trypsin, cells were suspended in PBS buffers with different pHs and analyzed by a FACScan cytometer. The fluorescence signals of FAM and TAMRA were respectively collected with their emission channels with excitation by a 488 nm laser.

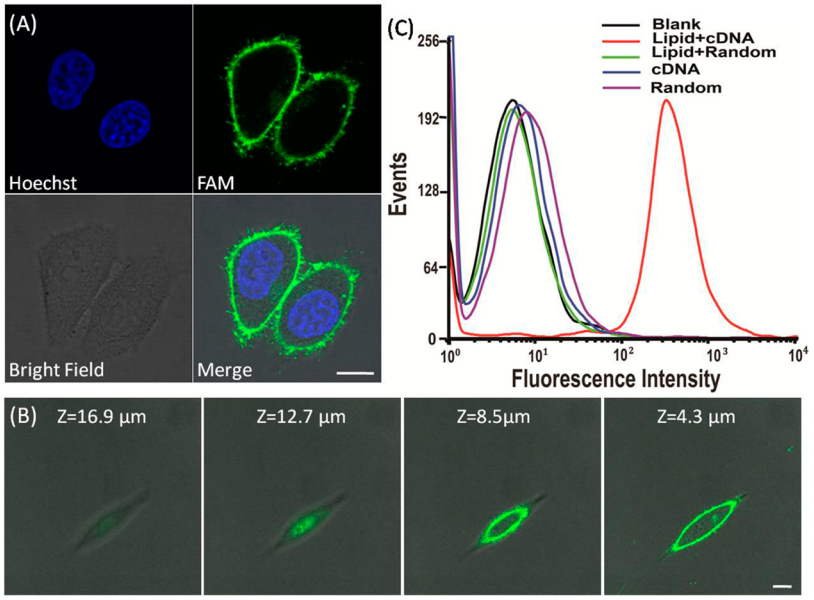

Figure 1. Location of lipid–DNA probes. (A) Confocal imaging of HeLa cells modified with FAM-labeled lipid–DNA probes and Hoechst 33258. (B) *z*-Scanning confocal imaging of Lipid-T_{20}-FAM-modified HeLa cells. (C) Flow cytometry experiment demonstrating the binding of FAM-labeled cDNA with Lipid-T_{20} on the cell membrane. The scale bar is 10 μm.

Extracellular pH Measurement of 3D Cell Cultures. HeLa cells were modified with mixed lipid–DNA probes as described above and redispersed in DMEM medium after digestion by trypsin/EDTA. An 80 μL aliquot of chilled 5 mg/mL type I collagen solution (Shengyou Biotechnology Co., Ltd., Hangzhou, China) was first added to 7 μL of 0.1 M NaOH and mixed immediately, followed by subsequent addition of 113 μL of 2× cold PBS buffer to adjust the pH of the solution to about 7.0. The mixed solution was added to 200 μL of HeLa cell suspension and placed in an incubator at 37 °C in 95% air/5% CO_2 for 1 h to form 3D cell cultures. Finally, the 3D sample was placed on a TCS SP5 confocal laser-scanning microscope for extracellular pH measurement. The pH in the 3D matrix was adjusted by addition of 1 M sodium phosphate monobasic solution and 1 M sodium phosphate dibasic solution.

RESULTS AND DISCUSSION

Working Principle of Cell-Anchored Lipid–DNA Probes for Extracellular pH Sensing. The working principle of our novel cell-surface-anchored DNA probes for extracellular pH sensing is illustrated in Scheme 1. The amphiphilic lipid–DNA probe consists of a hydrophobic diacyllipid tail, a hydrophilic DNA strand, and a pH-sensitive dye labeled on DNA. Due to the phospholipid bilayer structure of the cell membrane, lipid–DNA can be directly anchored on the membrane through the hydrophobic interaction between the hydrophobic lipid tail and the phospholipid.[20−22] The DNA strand extends out from the membrane because of its hydrophilic structure, thus ensuring that the pH-sensitive dye responds to the extracellular pH. For the purpose of ratiometric sensing of extracellular pH, two kinds of lipid–DNA probes labeled with a green-emission pH-sensitive dye (FAM) and an orange-emission pH-insensitive dye (TAMRA), respectively, are colocated on the cell membrane. As a result, the ratio of emission intensity of FAM versus TAMRA acts as the readout signal for extracellular pH sensing.

Anchoring of Lipid–DNA Probes on Cell Surface. To demonstrate the feasibility of using cell-anchored lipid–DNA probes for extracellular pH sensing, we first carried out flow cytometry and laser confocal imaging experiments to confirm the anchoring of the lipid–DNA probe on cell surface. In the confocal imaging experiment, HeLa cells were first cocultured with the FAM labeling lipid–DNA (Lipid-T_{20}-FAM) for 2 h and stained by nuclear staining dye Hoechst 33258 for 15 min. As shown in Figures 1A and S1 (Supporting Information), the fluorescence signal of Lipid-T_{20}-FAM probe came primarily from the cell membrane. In addition, the result of a *z*-axis depth scanning experiment also indicated that the green fluorescence in all *z*-axis planes came from the cell membrane (Figure 1B). These results provided strong evidence that the lipid–DNA was located on the cell membrane, which is in agreement with previous reports.[21,22]

To further study the behavior of the lipid–DNA probes, we performed the flow cytometry experiment. Cells labeled with nonfluorescent lipid–DNA probe (Lipid-T_{20}) were incubated with FAM-labeled complementary DNA strand (A_{20}-FAM) and FAM-labeled random DNA (Ran-FAM), respectively. As a control, cells without Lipid-T_{20} were also incubated with A_{20}-FAM and Ran-FAM, respectively. The results in Figure 1C show that cells modified with Lipid-T_{20} gained significant fluorescence enhancement after incubation with A_{20}-FAM due to the hybridization between sequence T_{20} and A_{20}. On the contrary, the fluorescence intensity of cells treated with Ran-FAM or without Lipid-T_{20} barely changes. Considering that it is difficult for negative-charged single-stranded DNA, such as A_{20}-FAM, to cross the negatively charged membrane without transfection reagents,[23] these results indicated that the diacyllipid tail anchors in the cell membrane with the DNA strand extending out for hybridization. The results clearly established the feasibility of lipid–DNA probes for biosensing on the cell membrane.

Other key properties of membrane-anchored lipid–DNA, including generality, cytotoxicity, and stability, were also investigated. Confocal imaging showed the successful modification of Lipid-T_{20}-FAM on the membranes of different types of cells, including human liver cancer cells QGY-7703, human liver normal cells QSG-7701, and human acute T cell leukemia cells Jurkat, thereby demonstrating the generality of the lipid–

DNA for different types of cells, including adherent cells and suspension cells, as well as normal cells and cancer cells (Figure 2A). The in vitro cell viability experiment (Figure 2B) showed

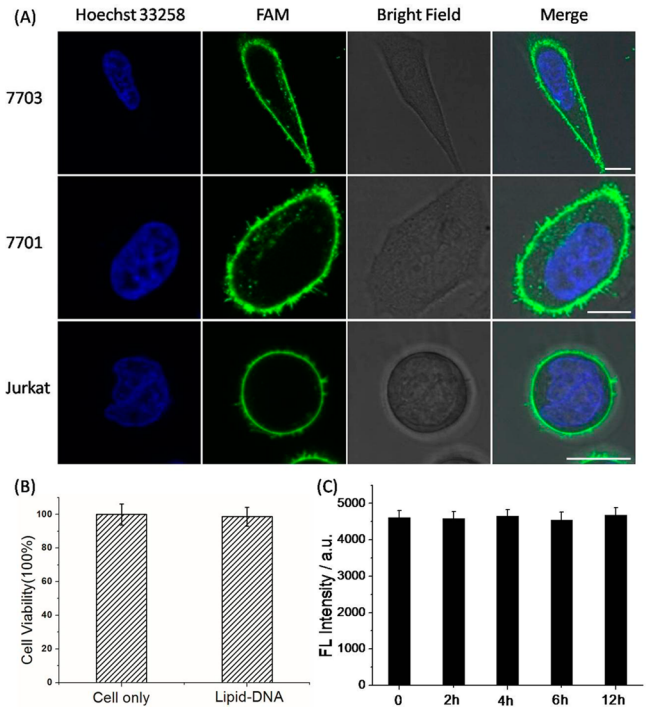

Figure 2. Performance of lipid–DNA probes. (A) Confocal fluorescence imaging of different cell types modified with Lipid-T_{20}-FAM probes and Hoechst 33258. The scale bar is 10 μm. (B) The in vitro cell viability of HeLa cells incubated with lipid–DNA probes. (C) Flow cytometry study of the fluorescence intensity at different time intervals of HeLa cells after modification with Lipid-T_{20}-FAM probes.

that our lipid–DNA is safe for cells at its working concentration (1 μM). Furthermore, the fluorescence intensity of cells with lipid–DNA remained almost the same, even after 12 h of culture (Figure 2C), indicating that anchoring of lipid–DNA on the cell membrane is stable and is, therefore, suitable for long-term monitoring.

Sensing pH in Buffer Using Lipid–DNA Probes. We first investigated the pH sensing performance of lipid–DNA probes in buffer. Our pH sensing lipid–DNA probes consist of FAM (pH-sensitive dye)-labeled Lipid-T_{20}-FAM and TAMRA (pH-insensitive dye)-labeled Lipid-T_{20}-TAMRA. Since the chemical structure of FAM varies as cation, neutral molecule, monoanion, or dianion at different pH values, the fluorescence intensity of FAM is pH-dependent in the range of 5.0–8.0,[24] while the fluorescence intensity of TAMRA remains almost the same at different pHs. The fluorescence intensity of mixed probes with 1:1 molar ratio in buffer monitoring extracellular environment was recorded for different pHs using a fluorescence spectrophotometer. As shown in Figures 3A and S2 (Supporting Information), the fluorescence intensity of TAMRA (λ_{ex} = 543 nm, λ_{em} = 580 nm) did not change in buffer with different pHs, while the fluorescence intensity of FAM (λ_{ex} = 488 nm, λ_{em} = 520 nm) was significantly enhanced as the pH increased from 5.8 to 8.0. The plot of emission intensity ratio of FAM versus TAMRA (F_{520nm}/F_{580nm}) and buffer pH (Figure 3B) shows that the ratio gradually increased with increasing pH. Moreover, as shown in Figure S3 (Supporting Information), the fluorescence intensity ratio of FAM versus TAMRA is consistent at the same pH, even at different concentrations. These results confirmed that dye labeling of lipid–DNA does not affect the capability of the dye to act as a pH indicator.

Extracellular pH Measurement. To demonstrate the applicability of the ratiometric extracellular pH sensors, we studied the response ratio for live HeLa cells treated with lipid–DNA as a function of extracellular pH. After incubation with lipid–DNA probes for 2 h, the cells were washed with PBS buffer to remove free probes in solution. Figure 4 shows the fluorescence intensity of HeLa cells in medium with different extracellular pHs. As shown in Figure 4A, a decrease in the extracellular pH led to a significant reduction of the emission intensity of FAM, while the fluorescence intensity of TAMRA barely changed, thereby significantly decreasing the FAM/TAMRA emission intensity ratio. The relationship between the emission ratio (FAM/TAMRA) and extracellular pH was obtained using ImageJ software (Figure 4B). The results show that the ratio increased as the extracellular pH increased, as observed for the response curve in PBS buffer. The pH-dependent fluorescence change of cells was also confirmed by flow cytometry. As shown in Figure 4C, although the fluorescence ratios from flow cytometry were slightly different from the results obtained by confocal imaging because of the different laser setup (note that, for confocal microscopy, the fluorescence of FAM and TAMRA were excited by 488 and 543

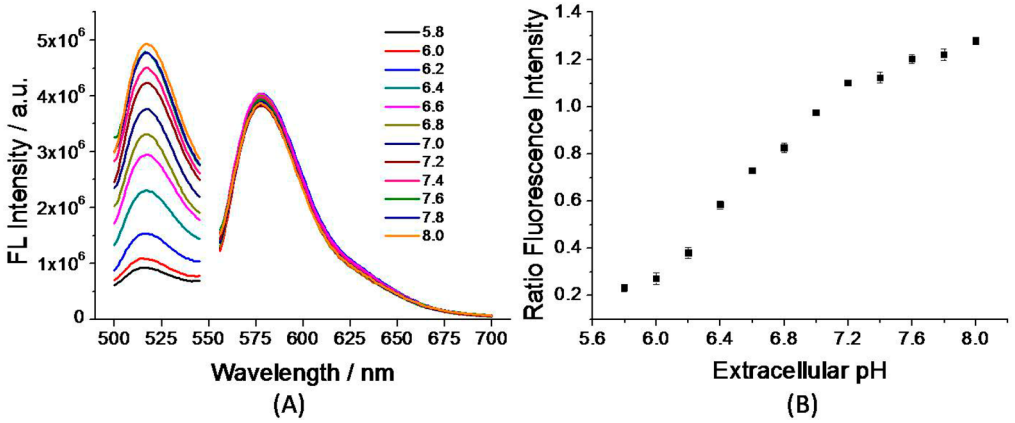

Figure 3. (A) The fluorescence spectrum (λ_{ex} = 488 nm, λ_{em} = 500–550 nm for FAM dye and λ_{ex} = 543 nm, λ_{em} = 555–700 nm for TAMRA dye) of mixed lipid–DNA probe in PBS buffer with different pHs. (B) Plot of fluorescence ratio (F_{520nm}/F_{580nm}) vs buffer pH.

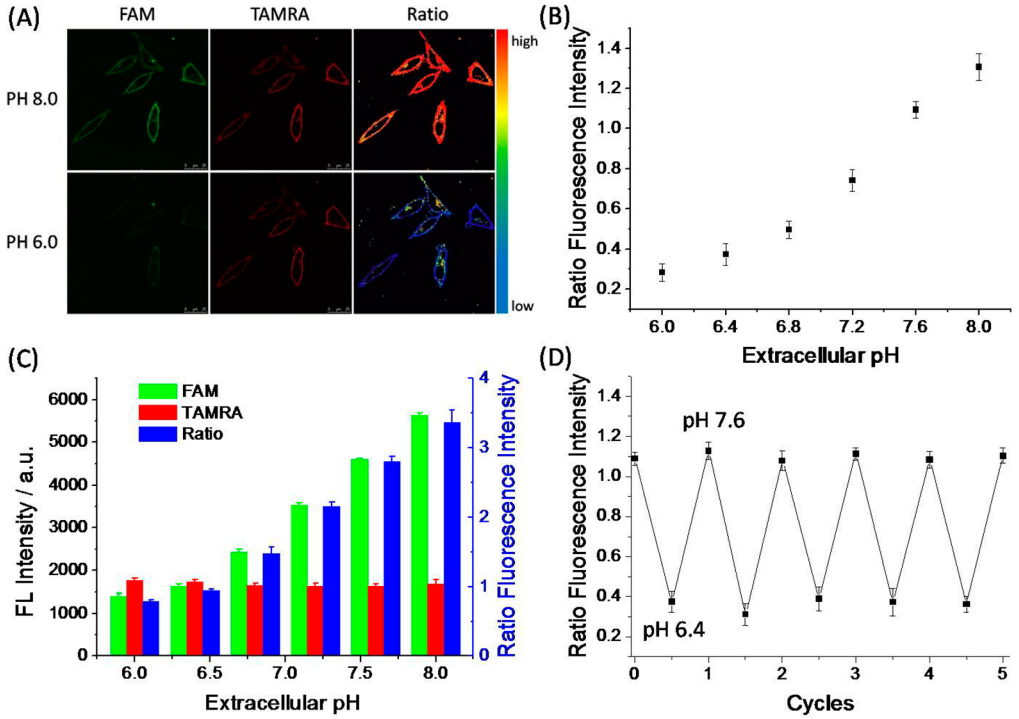

Figure 4. (A) Confocal fluorescence imaging of lipid–DNA-modified HeLa cells in different extracellular pHs. (B) Plot of emission intensity ratio (FAM/TAMRA) of HeLa cells modified with lipid–DNA probes vs extracellular pH. (C) Flow cytometry study of the response of the fluorescence intensity of HeLa cells modified with mixed lipid–DNA probes to different extracellular pHs. (D) The reversible change of fluorescence intensity ratio in response to extracellular pHs of 7.6 and 6.4.

nm lasers, respectively, while in flow cytometry, both FAM and TAMRA were excited at 488 nm), the overall trends of the emission ratio versus pH were similar for the two measurements. These results showed that our lipid–DNA probes enable ratiometric fluorescence analysis of extracellular pH using different fluorescent measurement methods. Moreover, the emission ratio responds reversibly to changes of extracellular pH (Figure 4D), thus making our lipid–DNA probes reusable during long-term monitoring or repeated pH cycling.

Application for Extracellular pH Measurement in a 3D Collagen Gel. The extracellular pH probe is an excellent potential tool for biomedical research and clinical tests. As an example, we utilized it for extracellular pH sensing of cells cultured in 3D collagen gel.[25] Research in past decades has shown that the morphologies and behaviors of cells in vivo are significantly different from those of cells cultured in a 2D plate.[26−28] By mimicking a 3D microenvironment in vivo, 3D cell culture has opened a new dimension for cell biologists.[29,30] However, unlike the simple and rapid substrate exchange in the culture medium in conventional 2D approaches, diffusion in a 3D culture medium is much more complex because of the limitations of the gel. This has become an obstacle for 3D studies, especially when the cellular microenvironment needs to be precisely controlled.[30,31] For example, the cell polarization relating to the cellular function and microenvironment variation under 3D culture conditions calls for precise monitoring of the change of the cellular microenvironment. Therefore, the effective monitoring of cellular environment, including extracellular pH, is significant in 3D cell-based research. To demonstrate the effectiveness of our small, cell-surface-anchored lipid–DNA probes for extracellular pH sensing in a 3D environment, our probes were successfully modified on the cell membranes of HeLa cells cultivated in 3D collagen gel and used for sensing extracellular pH changes. As shown in Figure 5, the emission ratio increased as the extracellular pH increased.

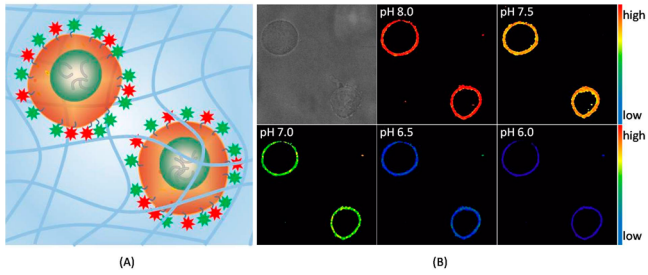

Figure 5. (A) Scheme for lipid–DNA-modified HeLa cells cultured in 3D collagen gel. (B) Bright-field imaging and ratio fluorescence imaging of HeLa cells in different extracellular pHs.

This result clearly demonstrated the feasibility of our lipid–DNA probe for extracellular pH sensing of 3D cells, making the probe a promising tool in 3D cell culture and study.

CONCLUSIONS

In conclusion, we have developed an amphiphilic lipid–DNA ratiometric probe for extracellular pH sensing. The amphiphilic lipid–DNA probe can be directly anchored on the cell surface with negligible cytotoxicity, excellent stability, and cell type universality because of hydrophobic interactions between the lipid tail and the cell membrane. Due to the inherent excellent properties of pH-sensitive FAM dye, the probes can sense extracellular pH with the advantages of rapid response, high sensitivity, and excellent reversibility. Moreover, the ratiometric readout strategy frees this probe from disturbance by the

complex biological environment, thus allowing excellent performance in extracellular pH measurement. With these advantages, the probe was successfully utilized for extracellular pH sensing of cells in 3D collagen gel, demonstrating the potential application of the probe in biology and medicine.[3,4]

■ ASSOCIATED CONTENT

Supporting Information

Confocal imaging of cells and fluorescence spectra of different concentrations of probes. This material is available free of charge via the Internet at http://pubs.acs.org.

■ AUTHOR INFORMATION

Corresponding Authors

*Tel: (+86) 592-218-7601. Fax: (+86) 592-218-9959. E-mail: cyyang@xmu.edu.cn.
*E-mail: zhuzhi@xmu.edu.cn.

Notes

The authors declare no competing financial interest.

■ ACKNOWLEDGMENTS

We thank the National Basic Research Program of China (2010CB732402, 2013CB933703), the National Science Foundation of China (91313302, 21205100, 21275122, 21075104), National Instrumentation Program (2011YQ03012412), the Fundamental Research Funds for the Central Universities (2012121025), NFFTBS(J1310024), and the National Science Foundation for Distinguished Young Scholars of China (21325522) for their financial support.

■ REFERENCES

(1) Lardner, A. The Effects of Extracellular pH on Immune Function. *J. Leukocyte Biol.* **2001**, *69*, 522−530.
(2) Arnett, T. R. Extracellular pH Regulates Bone Cell Function. *J. Nutr.* **2008**, *138*, 415S−418S.
(3) Zhang, X.; Lin, Y.; Gillies, R. J. Tumor pH and Its Measurement. *J. Nucl. Med.* **2010**, *51*, 1167−1170.
(4) Hashim, A. I.; Zhang, X.; Wojtkowiak, J. W.; Martinez, G. V.; Gillies, R. J. Imaging pH and Metastasis. *NMR Biomed.* **2011**, *24*, 582−591.
(5) Han, J.; Burgess, K. Fluorescent Indicators for Intracellular pH. *Chem. Rev.* **2010**, *110*, 2709−2728.
(6) Srivastava, J.; Barber, D. L.; Jacobson, M. P. Intracellular pH Sensors: Design Principles and Functional Significance. *Physiology* **2007**, *22*, 30−39.
(7) Chan, Y. H.; Wu, C.; Ye, F.; Jin, Y.; Smith, P. B.; Chiu, D. T. Development of Ultrabright Semiconducting Polymer Dots for Ratiometric pH Sensing. *Anal. Chem.* **2011**, *83*, 1448−1455.
(8) Chen, S.; Hong, Y.; Liu, Y.; Liu, J.; Leung, C. W.; Li, M.; Kwok, R. T.; Zhao, E.; Lam, J. W.; Yu, Y.; Tang, B. Z. Full-Range Intracellular pH Sensing by an Aggregation-Induced Emission-Active Two-Channel Ratiometric Fluorogen. *J. Am. Chem. Soc.* **2013**, *135*, 4926−4929.
(9) Tang, B.; Yu, F.; Li, P.; Tong, L.; Duan, X.; Xie, T.; Wang, X. A Near-Infrared Neutral pH Fluorescent Probe for Monitoring Minor pH Changes: Imaging in Living Hepg2 and Hl-7702 Cells. *J. Am. Chem. Soc.* **2009**, *131*, 3016−3023.
(10) Zhang, W.; Tang, B.; Liu, X.; Liu, Y.; Xu, K.; Ma, J.; Tong, L.; Yang, G. A Highly Sensitive Acidic pH Fluorescent Probe and Its Application to Hepg2 Cells. *Analyst* **2009**, *134*, 367−371.
(11) Surana, S.; Bhat, J. M.; Koushika, S. P.; Krishnan, Y. An Autonomous DNA Nanomachine Maps Spatiotemporal pH Changes in a Multicellular Living Organism. *Nat. Commun.* **2011**, *2*, 340.
(12) Marin, M. J.; Galindo, F.; Thomas, P.; Russell, D. A. Localized Intracellular pH Measurement Using a Ratiometric Photoinduced Electron-Transfer-Based Nanosensor. *Angew. Chem., Int. Ed.* **2012**, *51*, 9657−9661.
(13) Shi, W.; Li, X.; Ma, H. A Tunable Ratiometric pH Sensor Based on Carbon Nanodots for the Quantitative Measurement of the Intracellular pH of Whole Cells. *Angew. Chem., Int. Ed.* **2012**, *51*, 6432−6435.
(14) Wang, X. D.; Stolwijk, J. A.; Lang, T.; Sperber, M.; Meier, R. J.; Wegener, J.; Wolfbeis, O. S. Ultra-Small, Highly Stable, and Sensitive Dual Nanosensors for Imaging Intracellular Oxygen and pH in Cytosol. *J. Am. Chem. Soc.* **2012**, *134*, 17011−17014.
(15) Zhou, K.; Liu, H.; Zhang, S.; Huang, X.; Wang, Y.; Huang, G.; Sumer, B. D.; Gao, J. Multicolored pH-Tunable and Activatable Fluorescence Nanoplatform Responsive to Physiologic pH Stimuli. *J. Am. Chem. Soc.* **2012**, *134*, 7803−7811.
(16) Modi, S.; Nizak, C.; Surana, S.; Halder, S.; Krishnan, Y. Two DNA Nanomachines Map pH Changes along Intersecting Endocytic Pathways inside the Same Cell. *Nat. Nanotechnol.* **2013**, *8*, 459−467.
(17) Llopis, J.; McCaffery, J. M.; Miyawaki, A.; Farquhar, M. G.; Tsien, R. Y. Measurement of Cytosolic, Mitochondrial, and Golgi pH in Single Living Cells with Green Fluorescent Proteins. *Proc. Natl. Acad. Sci. U. S. A.* **1998**, *95*, 6803−6808.
(18) Tantama, M.; Hung, Y. P.; Yellen, G. Imaging Intracellular pH in Live Cells with a Genetically Encoded Red Fluorescent Protein Sensor. *J. Am. Chem. Soc.* **2011**, *133*, 10034−10037.
(19) Urra, J.; Sandoval, M.; Cornejo, I.; Barros, L. F.; Sepulveda, F. V.; Cid, L. P. A Genetically Encoded Ratiometric Sensor To Measure Extracellular pH in Microdomains Bounded by Basolateral Membranes of Epithelial Cells. *Pflugers Arch.* **2008**, *457*, 233−242.
(20) Liu, H.; Moynihan, K. D.; Zheng, Y.; Szeto, G. L.; Li, A. V.; Huang, B.; Van Egeren, D. S.; Park, C.; Irvine, D. J. Structure-Based Programming of Lymph-Node Targeting in Molecular Vaccines. *Nature* **2014**, *507*, 519−522.
(21) Liu, H.; Zhu, Z.; Kang, H.; Wu, Y.; Sefan, K.; Tan, W. DNA-Based Micelles: Synthesis, Micellar Properties and Size-Dependent Cell Permeability. *Chem.—Eur. J.* **2010**, *16*, 3791−3797.
(22) Xiong, X.; Liu, H.; Zhao, Z.; Altman, M. B.; Lopez-Colon, D.; Yang, C. J.; Chang, L. J.; Liu, C.; Tan, W. DNA Aptamer-Mediated Cell Targeting. *Angew. Chem., Int. Ed.* **2013**, *52*, 1472−1476.
(23) Giljohann, D. A.; Seferos, D. S.; Daniel, W. L.; Massich, M. D.; Patel, P. C.; Mirkin, C. A. Gold Nanoparticles for Biology and Medicine. *Angew. Chem., Int. Ed.* **2010**, *49*, 3280−3294.
(24) Sjoback, R. N. J.; Kubista, M. Absorption and Fluorescence Properties of Fluorescein. *Spectrochim. Acta, Part A* **1995**, *51*, L7−L21.
(25) Guan, Z. C.; Jia, S. S.; Zhu, Z.; Zhang, M. X.; Yang, C. J. Facile and Rapid Generation of Large-Scale Microcollagen Gel Array for Long-Term Single-Cell 3D Culture and Cell Proliferation Heterogeneity Analysis. *Anal. Chem.* **2014**, *86*, 2789−2797.
(26) Cukierman, E.; Pankov, R.; Stevens, D. R.; Yamada, K. M. Taking Cell-Matrix Adhesions to the Third Dimension. *Science* **2001**, *294*, 1708−1712.
(27) Elsdale, T.; Bard, J. Collagen Substrata for Studies on Cell Behavior. *J. Cell Biol.* **1972**, *54*, 626−637.
(28) Lutolf, M. P.; Hubbell, J. A. Synthetic Biomaterials as Instructive Extracellular Microenvironments for Morphogenesis in Tissue Engineering. *Nat. Biotechnol.* **2005**, *23*, 47−55.
(29) Pampaloni, F.; Reynaud, E. G.; Stelzer, E. H. K. The Third Dimension Bridges the Gap between Cell Culture and Live Tissue. *Nat. Rev. Mol. Cell Biol.* **2007**, *8*, 839−845.
(30) Yamada, K. M.; Cukierman, E. Modeling Tissue Morphogenesis and Cancer in 3D. *Cell* **2007**, *130*, 601−610.
(31) Tibbitt, M. W.; Anseth, K. S. Hydrogels as Extracellular Matrix Mimics for 3D Cell Culture. *Biotechnol. Bioeng.* **2009**, *103*, 655−663.